

# Maximal Acceleration Effects in Kerr Space.

V. Bozza<sup>a,b,\*</sup>, A. Feoli<sup>b,c,†</sup>, G. Lambiase<sup>a,b</sup>, G. Papini<sup>d,f,‡</sup>, G. Scarpetta<sup>b,e,f</sup>  
*<sup>a</sup>Dipartimento di Scienze Fisiche "E.R. Caianiello" Università di Salerno*  
*84081 - Baronissi - Salerno*

*<sup>b</sup>Istituto Nazionale di Fisica Nucleare, Sez. di Napoli, Italy.*

*<sup>c</sup>Facoltà d'Ingegneria, Università del Sannio*

*<sup>d</sup>Department of Physics, University of Regina,  
 Regina, Sask. S4S 0A2, Canada.*

*<sup>e</sup>Dipartimento di Fisica, Università di Salerno, 84081 Baronissi (Sa), Italy.*

*<sup>f</sup>International Institute for Advanced Scientific Studies,  
 Vietri sul Mare (Sa), Italy.*

December 17, 2018

## Abstract

We consider a model in which accelerated particles experience line-elements with maximal acceleration corrections that are introduced by means of successive approximations. It is shown that approximations higher than the first need not be considered. The method is then applied to the Kerr metric. The effective field experienced by accelerated test particles contains corrections that vanish in the limit  $\hbar \rightarrow 0$ , but otherwise affect the behaviour of matter greatly. The corrections generate potential barriers that are external to the horizon and are impervious to classical particles.

PACS: 11.17.+y; 04.62.+v

Keywords: Quantum Geometry, Maximal Acceleration, General Relativity.

---

\*E-mail: bozza,lambiase,scarpetta@sa.infn.it

†E-mail: feoli@unisannio.it

‡E-mail: papini@uregina.ca

This work is concerned with a geometrical model of quantum mechanics proposed by Caianiello [1]. The model interprets quantization as curvature of the relativistic eight-dimensional space-time tangent bundle  $TM = M_4 \otimes TM_4$  ( $M_4$  is the usual flat space-time manifold of metric  $\eta_{\mu\nu}$ ), satisfies the Born reciprocity principle and incorporates the notion that the proper accelerations of massive particles along their worldlines are normalized to an upper limit  $\mathcal{A}_m$  [2], referred to as maximal acceleration (MA). The value of  $\mathcal{A}_m$  can be derived from quantum mechanical considerations [3], [4]. Classical and quantum arguments supporting the existence of a MA have been frequently advanced [5],[6],[7]. MA also appears in the context of Weyl space [8] and of a geometrical analogue of Vigier's stochastic theory [9] and plays a role in numerous issues. It is invoked as a tool to rid black hole entropy of ultraviolet divergences [10] and of inconsistencies stemming from the application of the point-like concept to relativistic particles [11]. MA may be also regarded as a regularization procedure, alternative to those in which space-time is quantized by means of a fundamental length [12]. The advantage of Caianiello's proposal here lies in the preservation of the continuum structure of space-time.

An upper limit to the acceleration also exists in string theory where Jeans-like instabilities [13] occur [14] when the acceleration induced by the background gravitational field is large enough to render the string extremities causally disconnected. This critical acceleration  $a_c$  is determined by the string size  $\lambda$  and is given by  $a_c = \lambda^{-1} = (m\alpha)^{-1}$  where  $m$  is the string mass and  $\alpha^{-1}$  the usual string tension.

Frolov and Sanchez [15] have found that a universal critical acceleration  $a_c \simeq \lambda^{-1}$  must be a general property of strings. The acceleration cut-off is the same required by Sanchez in order to regularize the entropy and the free energy of quantum strings [16].

In all these instances the critical acceleration is a consequence of the interplay of the Rindler horizon with the finite extension of the particle. In Caianiello's proposal the maximal proper acceleration is a basic physical property of all massive particles, which is an inescapable consequence of quantum mechanics [3], [4], and must therefore be included in the physical laws from the outset. This requires a modification of the metric structure of space-time. It leads, in the case of Rindler space, to a manifold with a non vanishing scalar curvature and a shift in the horizon [17].

Applications of Caianiello's model include cosmology [18], where the initial singularity can be avoided while preserving inflation, the dynamics of accelerated strings [19], the energy spectrum of a uniformly accelerated particle [17] and neutrino oscillations [20],[21]. The model also makes the metric observer-dependent, as conjectured by Gibbons and Hawking [22].

The extreme large value that  $\mathcal{A}_m = 2mc^3/\hbar$  takes for all known particles makes a direct test of the model very difficult. Nonetheless a direct test that uses photons in a cavity has also been suggested [23].

We have worked out the consequences of the model for the classical electrodynamics of a particle [24], the mass of the Higgs boson [25] and the Lamb shift in hydrogenic atoms [26]. In the last instance the agreement between experimental data and MA corrections is very good for  $H$  and  $D$ . For  $He^+$  the agreement between theory and experiment is

improved by 50% when MA corrections are included.

MA effects in muonic atoms appear to be measurable [27]. MA also affects the helicity and chirality of particles [28].

More recently, we have applied the model to the falling of massive particles in the gravitational field of a spherically symmetric collapsing object [29]. In this problem MA manifests itself through a spherical shell external to the Schwarzschild horizon and impenetrable to classical particles. Massive, spinless bosons do not fare better [30]. Nor is the shell a sheer product of the coordinate system. It does survive, for instance, in isotropic coordinates. It is also present in the Reissner-Nordström case [31]. The usual process of formation of a black hole does not therefore appear viable in the model.

In this work we examine the possibility that the formation of the barrier at the horizon be a construct of the iteration procedure adopted [29],[30]. This is the first objective of the paper. The second objective deals with the angular momentum of the source which has so far been neglected. In fact, a collapsing object would very likely possess some angular momentum. One would then like to know whether some of the MA effects found persist in the case of the Kerr metric.

The embedding procedure introduced in [29] stipulates that the line element experienced by an accelerating particle is represented by

$$d\tau^2 = \left(1 + \frac{g_{\mu\nu}\ddot{x}^\mu\ddot{x}^\nu}{\mathcal{A}_m^2}\right) g_{\alpha\beta}dx^\alpha dx^\beta \equiv \sigma^2(x)g_{\alpha\beta}dx^\alpha dx^\beta. \quad (1)$$

As a consequence, the effective space-time geometry experienced by accelerating particles exhibits mass-dependent corrections that in general induce curvature and give rise to mass-dependent violations of the equivalence principle. The four-acceleration  $\ddot{x}^\mu = d^2x^\mu/ds^2$  appearing in (1) is a rigorously covariant quantity only for linear coordinate transformations. Though its transformation properties are known,  $\ddot{x}^\mu$  is in general neither covariant nor necessarily orthogonal to the four-velocity  $\dot{x}^\mu$ , as in Minkowski space. The justification for this choice lies primarily with the quantum mechanical derivation of  $\mathcal{A}_m$  which applies to  $\ddot{x}^\mu$ , is Newtonian in spirit (it requires the notion of force) and is only compatible with special relativity. No extension of this derivation to general relativity has so far been given. The choice of  $\ddot{x}^\mu$  in (1) is, of course, supported by the weak field approximation to  $g_{\mu\nu}$  which, to first order, is entirely Minkowskian. Estimates of  $\ddot{x}^\mu$  derived below assume that MA effects represent only perturbations of the normal particle motion represented by geodesics. These are described by fully covariant equations. In order to compare their results, any two observers would then determine each other's  $\ddot{x}^\mu$  and  $\sigma^2$  from their relative motion and the geodesics for a particle of the same mass in each other's frame. Lack of covariance is not therefore fatal in this respect. Other relevant points must be made. The model introduced is not intended to supplant general relativity, but only to provide a method to calculate the MA corrections to a Kerr line element. The effective gravitational field introduced in (1) can not be easily incorporated in general relativity (it violates, for one, the equivalence principle). Nor are the symmetries of general relativity indiscriminately applicable to (1). For instance, the

conformal factor is not an invariant, nor can it be eliminated by means of general coordinate transformations. The embedding procedure requires that it be present and that it be calculated in the same coordinates of the unperturbed gravitational background. On the other hand, Einstein's equivalence principle does not carry through readily to the quantum level [33], [34] and the same may be expected of its consequences, like the principle of general covariance [32]. Spectacular observer-dependent quantum mechanical effects are discussed by Gibbons and Hawking [22]. Complete covariance is, of course, restored in the limit  $\hbar \rightarrow 0$ , whereby all quantum corrections, including those due to MA, vanish. It is essential to keep these distinctions in mind in what follows.

The acceleration of a particle in Schwarzschild space diverges in proximity of the gravitational radius. A careful investigation of the embedding procedure is therefore necessary in order to better understand the validity of the approximation. For convenience, the units  $\hbar = c = G = 1$  are used below.

The Lagrangian of a particle in a metric isotropically conformal to that of Schwarzschild is

$$\mathcal{L} = -\frac{1}{2}\sigma^2(r) \left[ \left(1 - \frac{2M}{r}\right) \dot{t}^2 - \left(1 - \frac{2M}{r}\right)^{-1} \dot{r}^2 - r^2 \dot{\varphi}^2 \right] \quad (2)$$

and the 4-acceleration is

$$g_{\mu\nu} \ddot{x}^\mu \ddot{x}^\nu = F(r, \sigma^2(r)) , \quad (3)$$

where

$$\begin{aligned} F(r, \sigma^2(r)) = & \left\{ \left(1 - \frac{2M}{r}\right) \left[ \frac{2ME}{r^2 \left(1 - \frac{2M}{r}\right)^2 \sigma^2} + \frac{E}{\left(1 - \frac{2M}{r}\right) \sigma^4} \frac{d\sigma^2}{dr} \right]^2 \right. \\ & \left. - r^2 \left( \frac{2L}{r^3 \sigma^2} + \frac{L}{r^2 \sigma^4} \frac{d\sigma^2}{dr} \right)^2 \right\} \left[ \frac{E^2}{\sigma^4} - \left(1 - \frac{2M}{r}\right) \left( \frac{1}{\sigma^2} + \frac{L^2}{r^2 \sigma^4} \right) \right] \\ & - \frac{1}{\left(1 - \frac{2M}{r}\right)} \left\{ -\frac{M}{r^2 \sigma^2} + \frac{L^2}{r^3 \sigma^4} - \frac{3ML^2}{r^4 \sigma^4} - \left[ \frac{E^2}{\sigma^6} - \left(1 - \frac{2M}{r}\right) \left( \frac{1}{2\sigma^4} + \frac{L^2}{r^2 \sigma^6} \right) \right] \frac{d\sigma^2}{dr} \right\}^2 , \end{aligned} \quad (4)$$

$M$  is the mass of the source,  $E$  the energy of the particle and  $L$  its angular momentum. Setting  $\sigma^2 = 1$  in (3), one recovers the classical expression  $g_{\mu\nu} \ddot{x}_{(0)}^\mu \ddot{x}_{(0)}^\nu$  which is used in the first embedding to construct

$$\sigma_{(1)}^2(r) = \left( 1 + \frac{g_{\mu\nu} \ddot{x}_{(0)}^\mu \ddot{x}_{(0)}^\nu}{\mathcal{A}_m^2} \right) . \quad (5)$$

The dynamics generated by  $\sigma_{(1)}^2$  yields a new quantity  $g_{\mu\nu} \ddot{x}_{(1)}^\mu \ddot{x}_{(1)}^\nu$ , given by (3) with  $\sigma^2 = \sigma_{(1)}^2$ , which already contains the MA corrections and can be used to build the conformal factor of the second embedding

$$\sigma_{(2)}^2(r) = \left( 1 + \frac{g_{\mu\nu} \ddot{x}_{(1)}^\mu \ddot{x}_{(1)}^\nu}{\mathcal{A}_m^2} \right) . \quad (6)$$

Eq.(6) can then be used to calculate  $g_{\mu\nu}\ddot{x}_{(2)}^\mu\ddot{x}_{(2)}^\nu$  by means of (3), and so on. In particular

$$\sigma_{(n+1)}^2 = G\left(r, \sigma_{(n)}^2\right), \quad (7)$$

where

$$G\left(r, \sigma^2\right) = \left(1 + \frac{F\left(r, \sigma^2\right)}{\mathcal{A}_m^2}\right). \quad (8)$$

The effects of MA can be studied through the effective potential, defined by

$$\left(\frac{dr}{ds}\right)^2 = E^2 - V_{eff}^2. \quad (9)$$

One finds

$$V_{eff}^2\left(r, \sigma^2(r)\right) = E^2 - \frac{E^2}{\sigma^4(r)} + \left(1 - \frac{2M}{r}\right) \left(\frac{1}{\sigma^2(r)} + \frac{L^2}{r^2\sigma^4(r)}\right). \quad (10)$$

Eqs. (7), (8) and (4) give the successive embeddings with initial condition  $\sigma_{(0)}^2 = 1$ . The resulting effects on the dynamics of the particle can be analyzed numerically by means of (10). Fig.1a shows the classical effective potential for a particle with  $E = 1$  and  $L = 0$  in the region immediately external to the gravitational radius. Figs.1b, c, d show the effective potentials in the first, second and third embeddings respectively. In these plots the potential barrier of the first embedding disappears in the second, but reappears in the third. An analysis of the function  $G(r, \sigma^2)$  explains this behaviour. In the even embeddings,  $\sigma^2$  tends in fact to unity at  $r = 2M$ . The presence of inverse powers of  $\left(1 - \frac{2M}{r}\right)$  causes the odd  $\sigma^2$ 's to diverge as  $\left(1 - \frac{2M}{r}\right)^{-3}$ . Inversely, if  $\sigma^2$  diverges as  $\left(1 - \frac{2M}{r}\right)^{-3}$  in the odd embeddings, then  $F(r, \sigma^2)$  vanishes and  $\sigma^2$  is unity in the even embeddings. So the conformal factor alternates divergent to regular behaviour. Consequently,  $V_{eff}^2$  equals the classical potential in even embeddings and tends to  $E^2$  in the odd ones. This rules out any possibility that the iteration procedure converge at  $r = 2M$ . Fig.2 indicates that instability could even extend to outer regions in the form of an increasing, oscillating behaviour. This instability requires a closer study. *It will become clear below that the first embedding can be used as a good approximation in the model.* The starting point of the analysis is Eq. (7). If a new conformal factor is calculated by using the acceleration of a dynamics in which  $\sigma^2$  is the conformal factor, one must again find  $\sigma^2$ . Then the correct solution is characterized as a fixed point of (7). To gain information about the behaviour of  $\sigma^2$  at  $r = 2M$ , it is useful to inspect the divergence order. This is accomplished by writing

$$\sigma^2 = f(r) \left(1 - \frac{2M}{r}\right)^\alpha, \quad (11)$$

where  $f(r)$  is regular at  $r = 2M$ , and substituting (11) into the fixed point equation

$$\sigma^2 = G\left(r, \sigma^2\right). \quad (12)$$

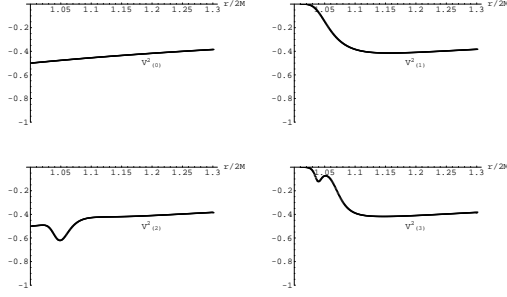


Figure 1: The classical potential  $V_{(0)}^2$  and the effective potentials from the first three embeddings.

Collecting terms with the same value of  $\alpha$ , the two sides of the equation are consistent with each other if and only if the divergence orders of the leading terms are the same. This condition is only fulfilled by  $\alpha = -\frac{3}{5}$ . If  $\sigma^2$  diverges, then the effective potential tends to  $E^2$  and the barrier forms. In order to get a complete view of the behaviour of the effective potential, one can resort to numerical algorithms. If one starts from any test value  $\tilde{\sigma}^2$ ,  $G(r, \tilde{\sigma}^2)$  indicates whether  $\tilde{\sigma}^2$  is greater or less than the "exact" solution  $\sigma^2$ . By decreasing the test value in the first case and increasing it in the second case, one can reach the exact  $\sigma^2$  with an arbitrary degree of accuracy. By building  $\sigma^2$  far from  $r = 2M$  so that  $\sigma^2 = 1$  is a good initial condition, one gradually approaches  $r = 2M$  always replacing derivatives with incremental ratios. In Fig.3 the effective potential resulting from this numerical approach is compared to the classical potential and the result of the first embedding for a particle with  $E = 1$  and  $L = 0$ . *The presence of a barrier at  $r = 2M$  is confirmed*, even though the lower degree of divergence of the exact  $\sigma^2$  with respect to  $\sigma_{(1)}^2$  produces a different behaviour near the horizon. To investigate the correct solution inside the Schwarzschild sphere, one must first overcome the divergence in  $\sigma^2$ . If one applies the same algorithm to  $\Sigma^2(r) = \frac{1}{\sigma^2(r)}$ , the divergence at  $r = 2M$  is replaced by zero and the interior of the black hole can be studied. Fig.4 compares the effective potentials for  $r < 2M$ . The singularity in the first embedding is absent in the exact numerical solution which instead has a simple minimum. Notice that the exact  $\sigma^2$  is everywhere positive while  $\sigma_{(1)}^2$  is negative between the singularity and  $2M$ . Finally, Fig.5 indicates that the exact potential does not vanish at  $r = 0$ . A plot of  $1/V_{eff}^2$  (Fig. 6) shows, in fact, that the correct function converges to a finite value.

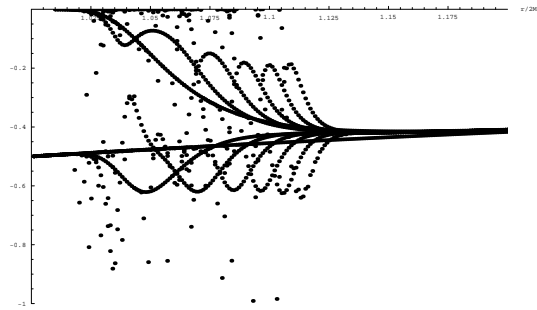


Figure 2: The oscillating behaviour of  $V_n^2$  up to  $n = 12$ .

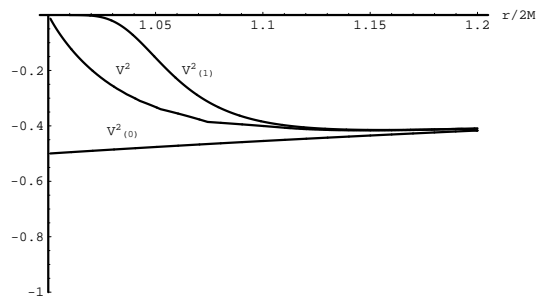


Figure 3: A numerical comparison of  $V^2$  with  $V_{(0)}^2$  and  $V_{(1)}^2$  for  $E = 1$  and  $L = 0$ .

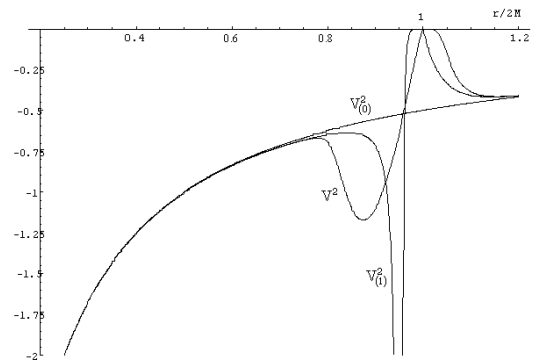


Figure 4: Classical and effective potentials inside the Schwarzschild sphere.

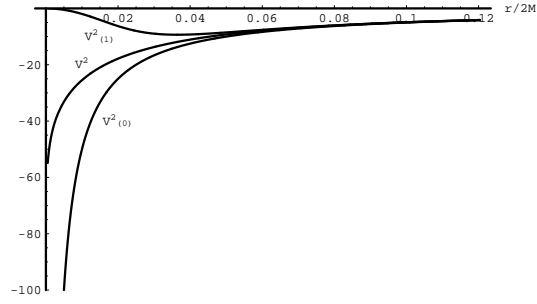


Figure 5: Behaviour of  $V^2_{(0)}$ ,  $V^2_{(1)}$  and  $V^2_{(2)}$  near the origin.

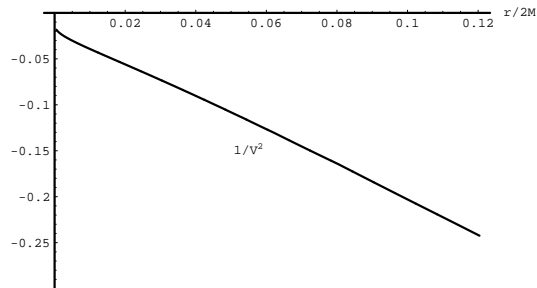


Figure 6: The plot of  $V^{-2}$  near the origin indicates that the exact effective potential  $V^2$  converges for  $r \rightarrow 0$ .



We now study the MA corrections to the radial motion of a particle in the Kerr metric. In polar coordinates, the line element of this space–time can be written in the form given by Boyer and Lindquist

$$d\tau^2 = \left(1 - \frac{2Mr}{\zeta^2}\right) dt^2 - \frac{\zeta^2}{\Delta} dr^2 - \zeta^2 d\theta^2 + \\ - \left(r^2 + a^2 + \frac{2Mra^2}{\zeta^2} \sin^2 \theta\right) \sin^2 \theta d\varphi^2 + \frac{4Mra}{\zeta^2} \sin^2 \theta dt d\varphi, \quad (13)$$

where  $\zeta^2 = r^2 + a^2 \cos^2 \theta$  and  $\Delta = r^2 - 2Mr + a^2$ . When  $a$  vanishes, the Schwarzschild geometry is recovered.

Three cases must be distinguished according to the possible values of  $a$  and  $M$ . When  $a < M$ , there are two null spherical surfaces of radii

$$r_{\pm} = M \pm \sqrt{M^2 - a^2}. \quad (14)$$

The external one is the event horizon. Particles can only enter, but not leave the interior of this shell. In the region  $r_+ < r < r_-$ , particles can only approach the origin, while at radii smaller than  $r_-$ , particles are again allowed to move away from the centre even if they can not re–emerge from  $r_-$ . Another characteristic feature of this metric is that the event horizon does not coincide with the static limit. This surface is given by the equation

$$r = M + \sqrt{M^2 - a^2 \cos^2 \theta} \quad (15)$$

and touches the event horizon at the two poles only. In the ergosphere the particles are compelled to rotate around the centre since no timelike geodesics exist for constant  $\varphi$ . For  $a = M$  the two null surfaces  $r_+$  and  $r_-$  merge into a single surface at  $r = M$ . The interior region is still inaccessible to external observers. Finally, for  $a > M$  there are no horizons and particles approaching the centre can always return. However, the structure of the Kerr metric allows closed timelike geodesics that violate causality for  $a \geq M$  and inside  $r_-$  for  $a < M$  [35, 36].

We investigate the effects of MA in all three cases and restrict the motion, for simplicity, to the plane  $\theta = \pi/2$ . Use can be made of the integrals of motion [35, 37]

$$\dot{t} = -\frac{2Ma}{r\Delta} \tilde{L} + \frac{\tilde{E}}{\Delta} \left(r^2 + a^2 + \frac{2Ma^2}{r}\right) \quad (16)$$

$$\dot{\varphi} = \frac{\tilde{L}}{\Delta} \left(1 - \frac{2M}{r}\right) + \frac{2Ma}{r\Delta} \tilde{E} \quad (17)$$

$$\dot{r}^2 = \frac{1}{r^4} \left[(r^2 + a^2) \tilde{E} - a\tilde{L}\right]^2 - \frac{\Delta}{r^4} \left[(a\tilde{E} - \tilde{L})^2 + r^2\right], \quad (18)$$

where  $\tilde{E}$  and  $\tilde{L}$  are the energy and angular momentum per unit of particle mass. These expressions depend on  $r$  only. In order to calculate the components of  $\ddot{x}^\mu$ , it is sufficient to take their derivatives with respect to  $r$  and multiply them by  $\dot{r}$ .  $\sigma^2$  can be

constructed according to (5) and then used to determine the dynamics of a particle with MA corrections. As explained above, only the first embedding needs to be considered.

The effective potential is defined by the equation

$$\left(\frac{dr}{ds}\right)^2 = \tilde{E}^2 - V_{eff}^2, \quad (19)$$

where the expressions for the momenta are derived, as usual [6], from the equation

$$\tilde{g}_{\mu\nu}p^\mu p^\nu = m^2, \quad (20)$$

and the definitions  $p^0 = mdt/ds$ ,  $p^1 = mdr/ds$ ,  $p^3 = md\phi/ds$ . In (20)  $\tilde{g}_{\mu\nu} = \sigma^2 g_{\mu\nu}$ .

The expression of  $V_{eff}^2$  for a particle moving in the equatorial plane of Kerr space-time is

$$V_{eff}^2 = \tilde{E}^2 - \frac{\tilde{E}^2}{\sigma^4(r)} + \frac{1}{\sigma^2(r)} \left(1 - \frac{2M}{r}\right) + \frac{\tilde{L}^2 - a^2\tilde{E}^2}{r^2\sigma^4(r)} - \frac{2M(\tilde{L} - a\tilde{E})^2}{r^3\sigma^4(r)} + \frac{a^2}{r^2\sigma^2(r)}. \quad (21)$$

When MA tends to infinity,  $\sigma^2(r) \rightarrow 1$  and the classical potential is recovered. In the limit of vanishing angular momentum ( $a \rightarrow 0$ ), one re-obtains the effective Schwarzschild potential previously studied [29].

The results for each one of the cases listed above are the following.

a)  $a < M$ . Fig. 7 (drawn for the values  $2M = 1$ ,  $a = 0.4$ ,  $\tilde{E} = 1$ ,  $\tilde{L} = 0$ ) shows that  $\tilde{V}_{eff}^2$  is not modified at the static limit  $r = 1$ , while potential barriers form at  $r_+ = 0.8$  and  $r_- = 0.2$ . These barriers are a consequence of the divergences of  $\sigma^2$  at the horizons. One finds that

$$\tilde{V}_{eff}^2(r) \sim \tilde{E}^2 + \frac{4r_+^2(r_+ - M)^2 m^2}{M^2[a\tilde{L} + \tilde{E}(a^2 + r_+^2)]^4} (r - r_+)^4$$

near  $r_+$  and tends to  $\tilde{E}^2$  at  $r_+$ . A particle coming from infinity cannot therefore pass through the event horizon.

In the region  $r_- < r < r_+$  each barrier is accompanied by a divergence that corresponds to a zero in  $\sigma^2$ . One more divergence can be found near the origin where the potential again approaches  $\tilde{E}^2$ .

Negative or low positive values of  $\tilde{L}$  do not alter the shape of the potential substantially. If  $\tilde{L}$  is higher than a certain threshold, two additional divergences appear outside the event horizon (Fig. 8). When  $\tilde{L} = a$ , the classical potential has a positive (instead of negative) divergence at the origin.  $\tilde{V}_{eff}^2$  is always regular at the origin, but the divergence near the origin becomes positive on the right side.

b) When  $a$  approaches  $M$ , the two horizons approach each other and so do the two barriers generated by MA. The two divergences accompanying them merge and disappear and only the two barriers are left, until they too merge when  $a = M$  (Fig.9). In this case all divergencies disappear and the potential is fully regularized.

We again obtain two divergences outside the horizon for high values of the angular momentum. For  $\tilde{L} = a$ , we find a divergence near the origin as in a).

c) When  $a > M$ , there are no horizons and the barrier shrinks until it disappears. In its place a negative divergence forms (Fig.10). The shape of the diagram remains substantially unaltered even for  $\tilde{L} \neq 0$ . For the particular value  $\tilde{L} = a$ , the effective potential is as in case b) (with  $\tilde{L} = a$ ).

It is remarkable that MA has no effect on particles passing through the static limit. The fact that particles in the ergosphere are bound to rotate does not lead to divergences in the conformal factor. Then particles enter and leave this region as they normally would in the absence of MA corrections.

Similarities in the structure of the Kerr and Reissner–Nordström [31] metrics are reflected in those of their effective potentials. There is a barrier on each null surface with a divergence in the region between the two horizons. If the incoming particle has an orbital angular momentum, nothing changes unless  $L$  coincides with the black hole angular momentum. Then the classical potential is strongly modified and the effective potential changes, but the barriers at the event horizons remain. When  $a > M$ , there are no more horizons and the barrier disappears, leaving a negative divergence that would be accessible to the external particles.

These results have a bearing on what discussed in [29]. In fact, in physical situations, collapsed bodies will likely have some angular momentum. One may then wonder whether angular momentum perturbations invalidate the results obtained for the Schwarzschild metric. This is not the case. The foregoing indicates that MA still produces a barrier at the horizon, even though the rotation of the black hole modifies the effective potential and the dynamics of the particles falling towards the event horizon. The barrier tends continuously to that of the Schwarzschild case and the fall of particles is halted. Hence the black hole cannot absorb new matter. In the model, the gravitational collapse of massive astrophysical objects is stopped before the occurrence of the event horizon. A black hole does not therefore form, at least in the traditional sense. However, a very compact radiating object would develop in its place, in appearance very similar to a black hole.

A black hole would nonetheless form if the accreting matter were first transformed into massless particles and these were absorbed by the collapsing object at a rate higher than the corresponding re-emission rate.

The results obtained represent a striking confirmation of and a decisive improvement upon the conclusions reached in [29]. The iteration of the embedding approach does not lead to a better approximation to the exact solution, because of the peculiar behaviour of the equation relating a new conformal factor to the previous one. Yet this instability does not affect the correctness of the first embedding which represents indeed the best approximation to the exact solution.

This not only applies to small accelerations, but even reproduces qualitatively the correct behaviour of the particle motion at the Schwarzschild radius. The occurrence of a potential barrier at the gravitational radius is confirmed by the exact solution. The

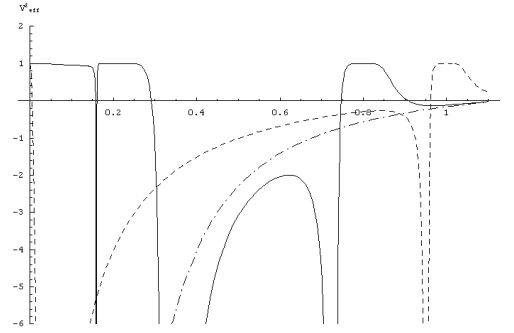


Figure 7: Potentials for  $\tilde{E} = 1$  and  $\tilde{L} = 0$  in a Kerr space with  $2M = 1$  and  $a = 0.4$ . Solid line: Effective potential with MA corrections. Dashed line: Schwarzschild potential with MA corrections. Dot-dashed line: Classical potential.

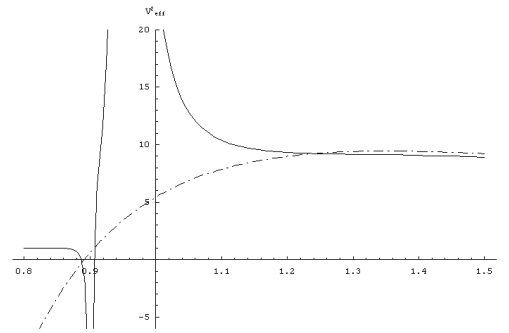


Figure 8: Potentials for  $\tilde{E} = 1$  and  $\tilde{L} = 7$  in a Kerr space with  $2M = 1$  and  $a = 0.4$ . Solid line: Effective potential with MA corrections. Dot-dashed line: Classical potential.

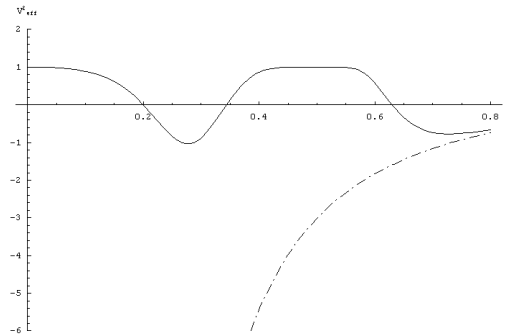


Figure 9: Potentials for  $\tilde{E} = 1$  and  $\tilde{L} = 0$  in a Kerr space with  $2M = 1$  and  $a = 0.5$ . Solid line: Effective potential with MA corrections. Dot-dashed line: Classical potential.

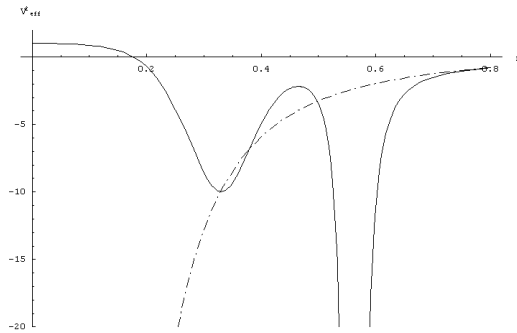


Figure 10: Potentials for  $\tilde{E} = 1$  and  $\tilde{L} = 0$  in a Kerr space with  $2M = 1$  and  $a = 0.53$ . Solid line: Effective potential with MA corrections. Dot-dashed line: Classical potential.

analysis of the motion of a particle moving radially towards the origin indicates that the proper time taken by the particle to reach the horizon is infinite. The particle would never fall into the black hole. The singularity in the approximate potential caused by a change of sign in  $\sigma_{(1)}^2$  is not present in the exact solution which is regular even at the origin. Apart from the classical shift from  $2M$  to  $r_+$ , the presence of angular momentum in a black hole essentially leaves the barrier at the external horizon unchanged. This means that all the remarks about the formation of black holes made in [29] with regard to the Schwarzschild metric can be extended to that of Kerr. The presence of the barrier would classically forbid, or at least slow-down, the formation of a black hole.

Beside confirming the dynamics of collapsing objects, the application of Caianiello's effective theory to the Kerr metric offers other interesting aspects. The structure of  $\tilde{V}_{eff}^2$  at the internal horizon  $r_-$  is the specular image of that at  $r_+$ . The intermediate region remains inaccessible from both sides. A barrier at a horizon is always accompanied by a singularity on the side where  $g_{00}$  is negative. These divergences are even present in the curvature invariants, so they must be considered as physical singularities of the effective metric. Unlike the Schwarzschild case, the singularity near the origin is always present because the repulsive effect of the central object's angular momentum preserves the behaviour of  $\sigma^2$  and  $\tilde{V}_{eff}^2$ . For high values of the angular momentum the divergence in the effective potential becomes positive and causes the formation of an infinite potential barrier. Though physical, these singularities remain inaccessible to massive particles and only regard the behaviour of matter inside the black hole, if the latter somehow formed. In the case  $a > M$  the barrier is directly accessible to particles coming from infinite distances and could play an important role in their dynamics.

### Acknowledgments

Research supported by MURST PRIN 99 and by the Natural Sciences and Engineering Research Council of Canada.

## References

- [1] E.R. Caianiello, Lett. Nuovo Cimento **25** (1979) 225; **27** (1980) 89; Il Nuovo Cimento **B59** (1980) 350; E.R. Caianiello, G. Marmo, and G. Scarpetta, Il Nuovo Cimento **A 86** (1985) 337; E.R. Caianiello, La Rivista del Nuovo Cimento **15** n.4 (1992) and references therein.
- [2] E.R. Caianiello, Lett. Nuovo Cimento **32**(1981) 65; E.R. Caianiello, S. De Filippo, G. Marmo, and G. Vilasi, Lett. Nuovo Cimento **34** (1982) 112.
- [3] E.R. Caianiello, Lett. Nuovo Cimento **41** (1984) 370.
- [4] W.R. Wood, G. Papini and Y.Q. Cai, Il Nuovo Cimento **B104**, 361 and (errata corrige) 727 (1989).
- [5] A. Das, J. Math. Phys. **21** (1980) 1506;  
M. Gasperini, Astrophys. Space Sci. **138** (1987) 387;  
M. Toller, Nuovo Cimento **B102** (1988) 261; Int. J. Theor. Phys. **29** (1990) 963;  
Phys. Lett. **B256** (1991) 215;  
B. Mashhoon, Physics Letters **A143** (1990) 176;  
V. de Sabbata, C. Sivaram, Astrophys. Space Sci. **176** (1991) 145; *Spin and Torsion in gravitation*, World Scientific, Singapore, (1994);  
D.F. Falla, P.T. Landsberg, Il Nuovo Cimento **B 106**, (1991) 669;  
A.K. Pati, Il Nuovo Cimento **B 107** (1992) 895; Europhys. Lett. **18** (1992) 285.
- [6] C.W. Misner, K.S. Thorne, J. A. Wheeler, *Gravitation*, W.H. Freeman and Company, S. Francisco, 1973.
- [7] H.E. Brandt, Lett. Nuovo Cimento **38**, (1983) 522; Found. Phys. Lett. **2** (1989) 3.
- [8] G. Papini and W.R. Wood, Phys. Lett. **A170** (1992) 409; W.R. Wood and G. Papini, Phys. Rev. **D45** (1992) 3617; Found. Phys. Lett. **6** (1993) 409; G. Papini, Mathematica Japonica **41** (1995) 81.
- [9] J. P. Vigièr, *Found. Phys.* 21 (1991) 125.
- [10] M. McGuigan, Phys. Rev. **D50** (1994) 5225.
- [11] G.C. Hegerfeldt, Phys. Rev. **10 D** (1974) 3320.
- [12] See, for instance: J.C. Breckenridge, V. Elias, T.G. Steele, Class. Quantum Grav. **12** (1995) 637.
- [13] N. Sanchez and G. Veneziano, Nucl. Phys. **333 B**, (1990) 253;  
M. Gasperini, N. Sanchez, G. Veneziano, Nucl. Phys., **364 B** (1991) 365; Int. J. Mod. Phys. **6 A** (1991) 3853.

- [14] M. Gasperini, Phys. Lett. **258 B** (1991) 70; Gen. Rel. Grav. **24** (1992) 219.
- [15] V.P. Frolov and N. Sanchez. Nucl. Phys. **349 B** (1991) 815.
- [16] N. Sanchez, in “*Structure: from Physics to General Systems*” eds. M. Marinaro and G. Scarpetta (World Scientific, Singapore, 1993) vol. 1, pag. 118.
- [17] E.R. Caianiello, A. Feoli, M. Gasperini, G. Scarpetta, Int. J. Theor. Phys. **29** (1990) 131.
- [18] E.R. Caianiello, M. Gasperini, G. Scarpetta, Class. Quantum Grav. **8** (1991) 659; M. Gasperini, in “Advances in Theoretical Physics” ed. E.R. Caianiello, (World Scientific, Singapore, 1991), p. 77.
- [19] A. Feoli, Nucl. Phys. **B396** (1993) 261.
- [20] E.R. Caianiello, M. Gasperini, and G. Scarpetta, Il Nuovo Cimento **B105** (1990) 259.
- [21] V. Bozza, G. Lambiase, G. Papini, G. Scarpetta, Phys. Lett. **A279** (2001) 163.
- [22] G. Gibbons and S.W. Hawking, Phys. Rev. **D15** (1977) 2738.
- [23] G. Papini, A. Feoli, and G. Scarpetta, Phys. Lett. **A202** (1995) 50.
- [24] A. Feoli, G. Lambiase, G. Papini, and G. Scarpetta, Il Nuovo Cimento **112B** (1997) 913.
- [25] G. Lambiase, G. Papini, and G. Scarpetta, Il Nuovo Cimento **114B** (1999) 189. See also S. Kuwata, Il Nuovo Cimento **111B** (1996) 893.
- [26] G. Lambiase, G. Papini, and G. Scarpetta, Phys. Lett. **244A** (1998) 349.
- [27] C.X. Chen, G. Lambiase, G. Mobed, G. Papini, and G. Scarpetta, Il Nuovo Cimento **B114** (1999) 1135.
- [28] C.X. Chen, G. Lambiase, G. Mobed, G. Papini, and G. Scarpetta, Il Nuovo Cimento **B114** (1999) 199.
- [29] A. Feoli, G. Lambiase, G. Papini, G. Scarpetta, Phys. Lett. **A263** (1999) 147.
- [30] S. Capozziello, A. Feoli, G. Lambiase, G. Papini, G. Scarpetta, Phys. Lett. **A268** (2000) 247.
- [31] V. Bozza, A. Feoli, G. Papini, G. Scarpetta, Phys. Lett. **A271**(2000)35.
- [32] S. Weinberg, ”Gravitation and Cosmology”, John Wiley and Sons, New York, 1972, Ch.4.

- [33] C. Lämmerzahl, Gen. Rel. Grav. **28**(1996)1043.
- [34] D. Singh and G. Papini, Il Nuovo Cimento **B115**(2000)223.
- [35] B. Carter, Phys. Rev., **174** (1968)1559.
- [36] S.W. Hawking, G.F. Ellis, “The large scale structure of space–time”, Cambridge University Press, 1973.
- [37] L.D. Landau, E.M. Lifshits, “The Classical Theory of Fields”, Pergamon Press, Oxford, 1975.